Electronic Supplementary Material (ESI) for Journal of Materials Chemistry B.

Electronic Supporting Information

Understanding the Contribution of Surface Roughness and Hydrophobic Modification on Silica Nanoparticles for Enhanced Therapeutic Protein Delivery

Yuting Niu,[a] Meihua Yu, [a] Anand Meka, [a] Yang Liu, [a] Jun Zhang, [a] Yannan Yang, [a] and Chengzhong Yu*,[a]

Australian Institute for Bioengineering and Nanotechnology, the University of Queensland, Brisbane, QLD 4072, Australian. Fax: +61-7-334 63973; Tel: +61-7-334 63283; E-mail: c.yu@uq.edu.au

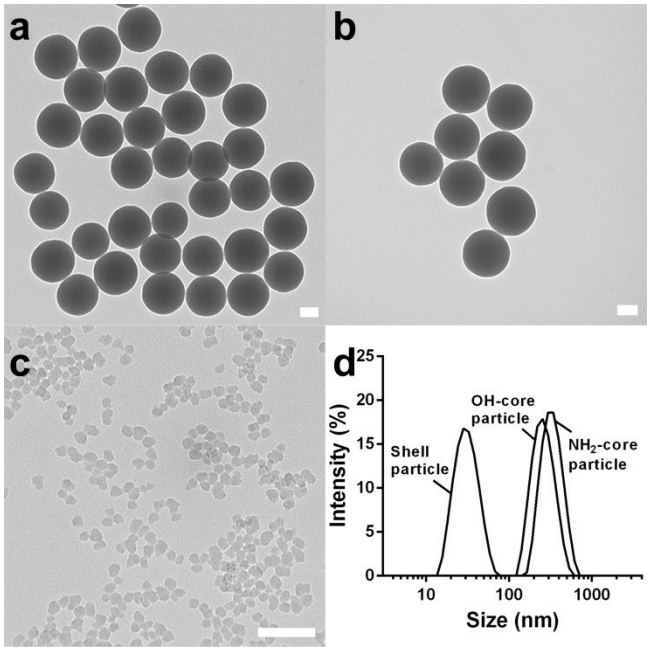

Figure S1. TEM images of (a) OH-core particle, (b) NH_2-core particle and (c) shell particle. Scale bar: 100 nm. (d) Particle size distribution curves measured by DLS.

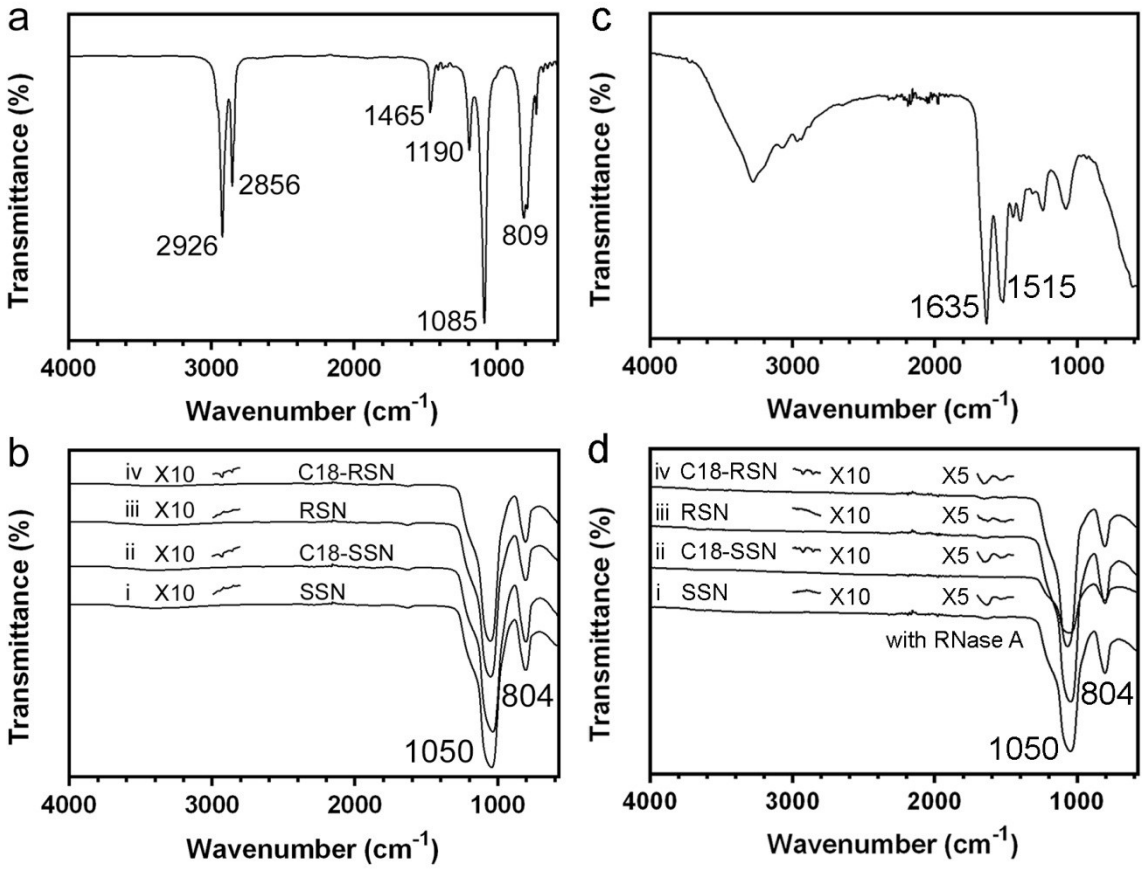

Figure S2. Fourier transform infrared (FTIR) spectra of (a) pure liquid OTMS, (b) bare nanoparticles, (c) RNase A and (d) nanoparticles complexed with RNase A.

The nanoparticles with and without modification of octadecyl group was characterized by FTIR technique. Figure S2a shows the FTIR spectrum of pure liquid OTMS, in which the characteristic peaks at 809, 1085, 1190, 1465, 2856 and 2926 cm^{-1} can be attributed to ν(Si-O), ν(C-O)+ ν(C-C), ρ(CH_3), δ(C-H) [1] and symmetric and anti-symmetric -CH_2- stretching,[2, 3] respectively. The spectra of SSN (Figure S2b i), C18-SSN (Figure S2b ii), RSN (Figure S2b iii) and C18-RSN (Figure S2b iv) show the same characteristic bands at 804 cm^{-1} and broad band peaked at 1050 cm^{-1}, which indicate -Si-O-Si- bonding.[4] In the spectra of hydrophobic modified silica nanoparticles (Figure S2b ii & iv), besides the characteristic peaks of silica, two extra peaks at 2858 and 2929 cm^{-1} can be observed, which are assigned to symmetric and anti-symmetric -CH_2- stretching, respectively, indicating the successful attachment of octadecyl-groups.[5]

Figure S2c exhibits the FTIR spectrum of RNase A. The characteristic amide I band centered at ~1635 cm^{-1} is mainly attributed to C O stretching vibration and the amide II band centered at ~1515 cm^{-1} can be assigned to in-plane N-H bending and C-N stretching.[6, 7] After RNase A adsorption onto silica nanoparticles, the two characteristic peaks of RNase A at 1635 and 1515 cm^{-1} can be clearly observed (Figure S2d). SSN (Figure S2d i) and RSN (Figure S2d iii) also show characteristic peaks of silica, while C18-SSN (Figure S2d ii) and C18-RSN (Figure S2d

iv) show additional characteristic peaks of silica and octadecyl-groups. These results suggest RNase A molecules have been successfully loaded onto the four samples.

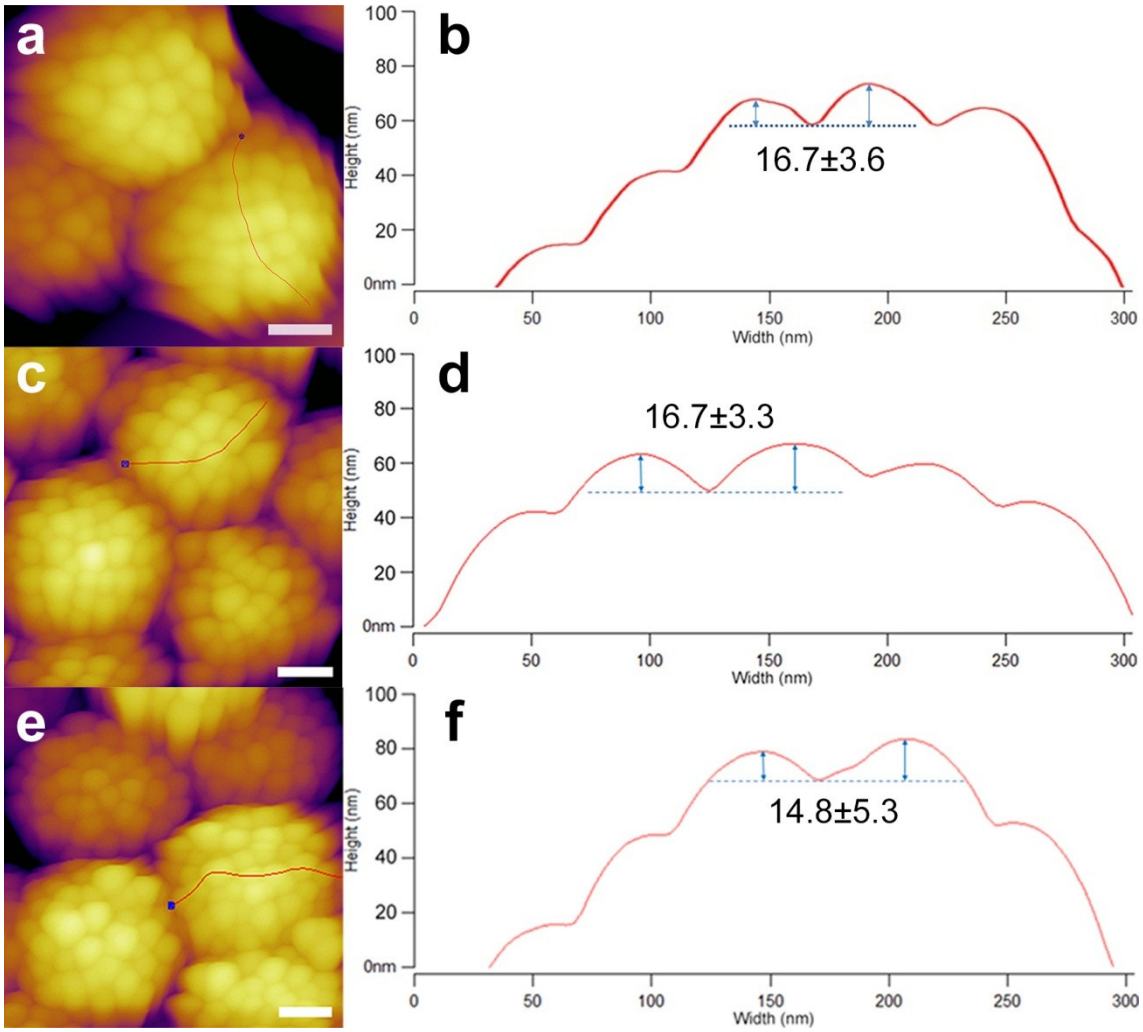

Figure S3. (a, c, e) AFM images and (b, d, f) void height profiles of (a & b) RSN, (c & d) C18-RSN and (e & f) C18-RSN + RNase A, generated by drawing a typical cross-sectional line on the top region, Scale bar: 100 nm. The average height values are measured and calculated by recording 20 data. Data represent mean ± SD.

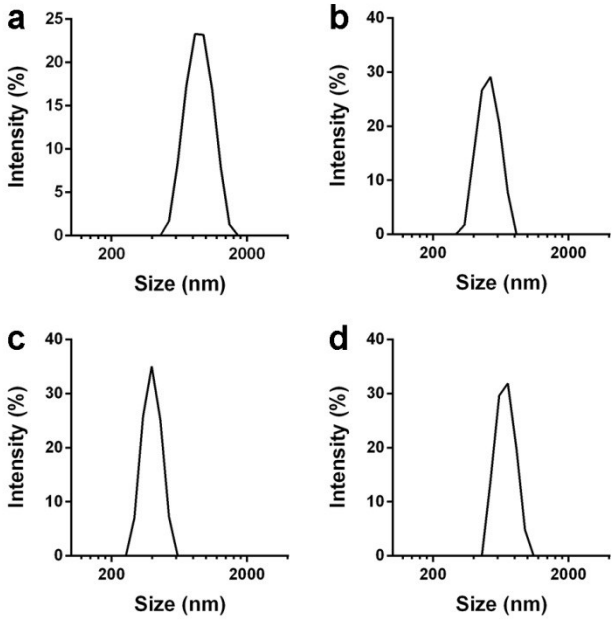

Figure S4. Particle size distribution curves of (a) SSN, (b) C18-SSN, (c) RSN and (d) C18-RSN.

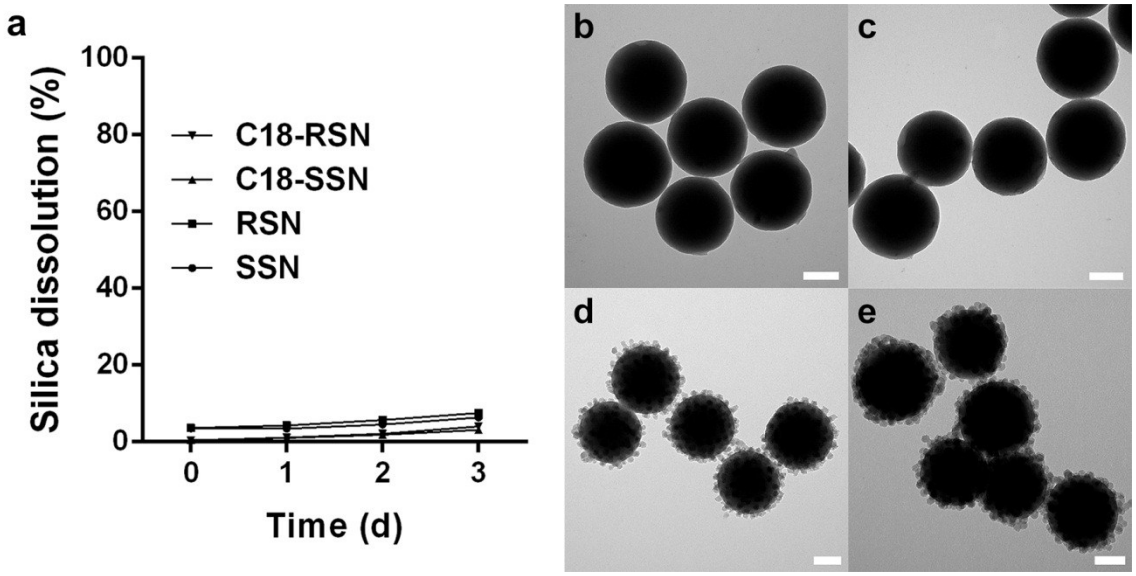

Figure S5. Silica dissolution of different nanoparticles, tested by (a) ICPOES and TEM images of (b) SSN, (c) C18-SSN, (d) RSN and (e) C18-RSN, after shaking in PBS for 3 days. Scale bar: 100 nm.

SSN, RSN, C18-SSN and C18-RSN show good stability in PBS with silica dissolution percentages less than 10% after 3 days (Figure S5a). Slight increases in the silica dissolution percentage are observed in four samples as shaking time increases. After 3 days, RSN and C18-RSN exhibit relatively higher silica dissolution percentages (7.6% and 4.1%), compared to SSN and C18-SSN (6.4% and 3.1%), respectively. This can be explained by the larger surface area of rough nanoparticles, which facilitates quicker interaction with medium and subsequent silica dissolution. In addition, the hydrophobic layer has an obvious protection effect to reduce silica dissolution. The stability of nanoparticles was further confirmed by TEM images, where the surface morphologies of both smooth (Figure S5b&c) and rough nanoparticles (Figure S5d&e) were not significantly affected after shaking in PBS for 3 days.

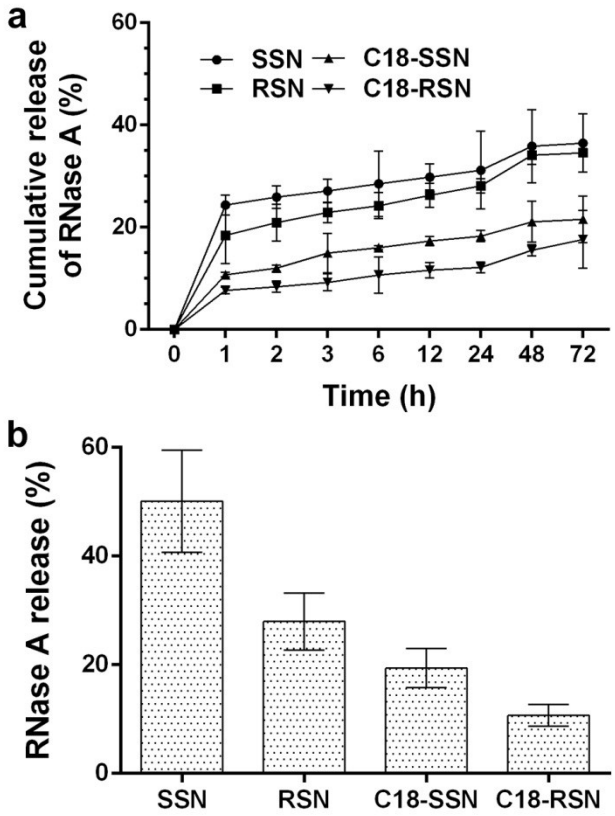

Figure S6. RNase A release profiles of SSN, RSN, C18-SSN and C18-RSN at (a) acidic condition (pH 4.5) and (b) in DMEM under static condition at 37 °C for 4 h. Data represent mean±SD.

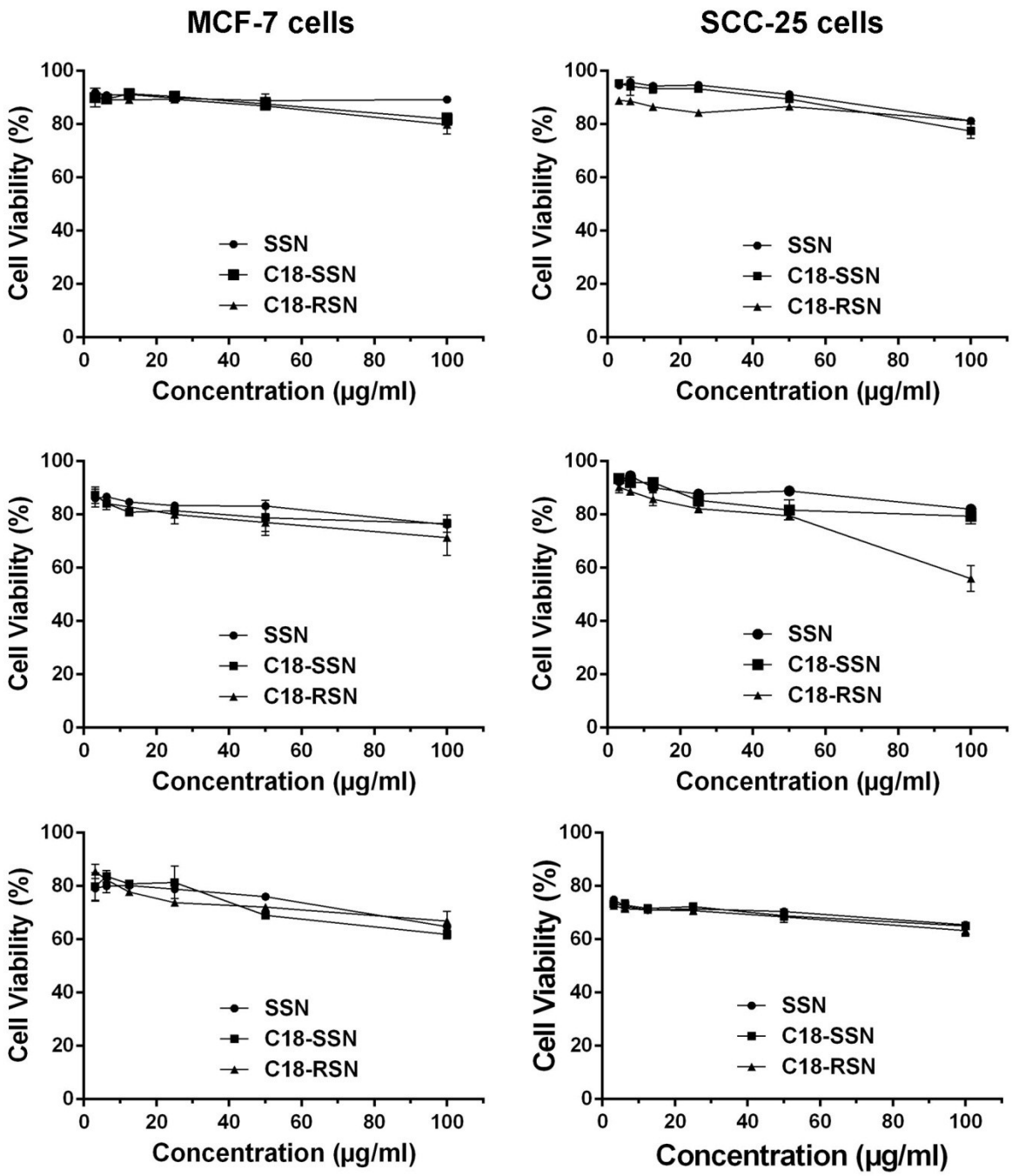

Figure S7. The evaluation of toxicity from pure nanoparticles (a,c,e) in MCF-7 cells and (b,d,f) in SCC-25 cells, at 24 h, 48 h and 72 h, respectively. Data represent mean ± SD.

Table S1. Size and ζ potential characterizations of nanoparticles.

Sample ID	Size		PDI[c]	ζ-potential
	TEM[a]	DLS[b]		
Shell particle	20±2.4	34±0.6	0.07±0.01	-42±8.3
OH-core particle	232±9.6	281±10.4	0.13±0.03	-24±1.3
NH_2-core particle	235±10.9	328±11.5	0.24±0.09	+38±0.9
SSN	240±9.3	324±10.3	0.30±0.07	-34±0.4
C18-SSN	240±17.5	277±7.0	0.03±0.03	-33±0.5
RSN	296±10.0	630±44.3	0.23±0.01	-22±0.7
C18-RSN	299±14.6	499±42.6	0.16±0.01	-22±0.6

[a] Mean size±SD of shell/core particles by recording 50 data from TEM images. [b] Intensity mean size ±SD of shell/core particles by DLS method. [c] Polydispersity index.

Table S2. DLS size measurements in PBS.

Sample ID	Size[a]	PDI[b]
SSN	391±68.1	0.40±0.05
C18-SSN	599±111.3	0.31±0.01
RSN	512±158.2	0.43±0.01
C18-RSN	683±12.9	0.30±0.01

[a] Intensity mean size ±SD of shell/core particles by DLS method. [b] Polydispersity index.

Table S3. RNase A adsorption density and C18-modification characterization of nanoparticles

Sample ID	$D_{RNase\ A}$[a] (mg/m^2)	Carbon (%)[b]	D_{C18}[c] ($\mu mol/m^2$)
SSN	0.56	0.011	--
C18-SSN	0.81	0.453	1.61
RSN	0.61	0.025	--
C18-RSN	0.95	1.274	2.42

[a] RNase A adsorption density

[b] Carbon percentage tested by Elemental Analysis.

[c] Octadecyl-group (C18) -group density: C18-group amount per unit surface area. The molecular weight of C18 (MW_{C18}) is 236g/mol. SSN and RSN were used as control group.

$$C18\ density = \frac{Carbon\ (\%)}{S_{BET} \times MW_{C18}} \quad (1)$$

References

1 M. I. Tejedor-Tejedor, L. Paredes and M. A. Anderson, *Chem. Mater*, 1998, **10**, 3410-3421.

2 H. Huang, Y. Ji, Z. Qiao, C. Zhao, J. He and H. Zhang, *J. Autom. Methods Manag. Chem.*, 2010, **2010**, 7.

3 K. Kailasam and K. Muller, *J. Chromatogr A*, 2008, **1191**, 125-135.

4 D. B. Mahadik, A. V. Rao, A. P. Rao, P. B. Wagh, S. V. Ingale and S. C. Gupta, *J. Colloid Interf Sci*, 2011, **356**, 298-302.

5 J. Zhang, S. Karmakar, M. H. Yu, N. Mitter, J. Zou and C. Z. Yu, *Small*, 2014, **10**, 5068-5076.

6 P. Roach, D. Farrar and C. C. Perry, *J. Am. Chem. Soc.*, 2006, **128**, 3939-3945.

7 C. l. Chadefaux, A.-S. L. H£¿, L. Bellot-Gurlet and I. Reiche, *E-Preservation Science*, 2009, **6**, 129-137.